Development of components of the optical path for Thomson scattering diagnostics located on tokamak ITER divertor cassettes

© N.A. Kungurtsev[1], A.N. Koval[1], E.E. Mukhin[1], S.Yu. Tolstyakov[1], A.G. Razdobarin[1], D.I. Elets[1], O.S. Medvedev[1], I.M. Bukreev[1], K.O. Nikolaenko[1], I.D. Kirienko[2], A.A. Zhadkovskij[2], V.I. Modestov[2], D.L. Bogachev[3]

[1] Peter the Great Saint-Petersburg Polytechnic University, St. Petersburg, Russia
[3] Spectral-Tech, St. Petersburg, Russia
E-mail: n.a.kungurtsev@mail.ioffe.ru

Received May 5, 2025
Revised June 28, 2025
Accepted July 18, 2025

The diagnostic components of Thomson scattering (TS) placed on ITER divertor cassettes are exposed to radiation, radiation heating, exposure to a strong magnetic field of 6–9 T, as well as shock effects from the interaction of a permanent magnetic field with eddy currents induced in structures during plasma discharge failures. The article discusses the design features of components that allow them to remain operational in close proximity to thermonuclear plasma, fulfilling specific diagnostic requirements.

Keywords: ITER, Thomson scattering, laser radiation, divertor.

DOI: 10.61011/TPL.2025.12.62786.7891

Thomson scattering diagnostics in ITER tokamak divertor plasma is included in the list of diagnostic systems that should be operational at the FPO-1 (FPO — first plasma operation) stage of phase DT-1 (DT — deuterium-tritium). It supports measurements of the dynamics of spatial distributions of electron temperature $T_e(r,t)$ and concentration $n_e(r,t)$ for control over the discharge regimes [1]. Another functional purpose of the diagnostics is to prepare a $T_e(r,t)/n_e(r,t)$ database for analysis of physical processes and development of reliable models and codes for plasma parameter calculation. In 2024, designs of diagnostic components located on the divertor cassettes, which are to be installed in the tokamak at the preliminary SRO (start of research operation) phase, have been presented as part of the first stage of the final project for Thomson scattering diagnostics at the ITER divertor. The list of diagnostic components located on the divertor cassettes includes a passive protection system for the laser radiation input device (a gasdynamic protection device), bottom and top shadow screens for shielding the scattered radiation collection system from glow of the surface of the heated internal divertor target, and a laser radiation dump (Fig. 1). Their integrity determines the performance of the diagnostics system, which provides data that may be used in the control system. If these components are lacking, the operation of the tokamak reactor itself may ultimately be affected. All designs were devised with account for the topological requirements of cassette installation, ensure access during assembly, and provide the required temperature decoupling of molybdenum parts and steel structures of the divertor cassettes.

Particular attention was paid to the thermal interface between the components and the cassette and to unloading of welded joints. A complete set of strength analyses was performed for the developed designs in the ANSYS software package. All possible load combinations for the normal tokamak operating mode and for the mode introducing possible incidents in operation were taken into account. The greatest challenge was to design the screens located under the dome of the divertor cassettes. Extreme thermal loads are combined at this site with the required minimization of temperature of surfaces within the field of view of the scattered radiation collection system. In addition, the use of a molybdenum alloy, which is distinguished by high thermal conductivity, is combined with the need to take its radiation embrittlement into account.

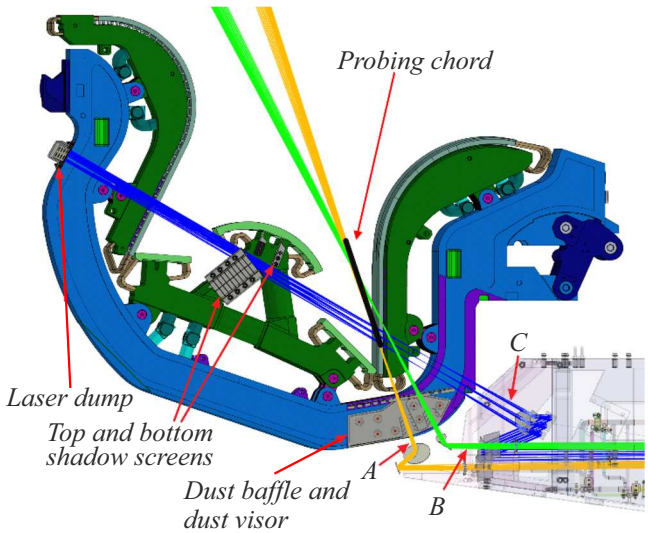

Figure 1. Diagnostic components located on divertor cassettes 21 and 22. Laser probing chords with the first laser mirrors marked with arrows *A*, *B*, and *C*.

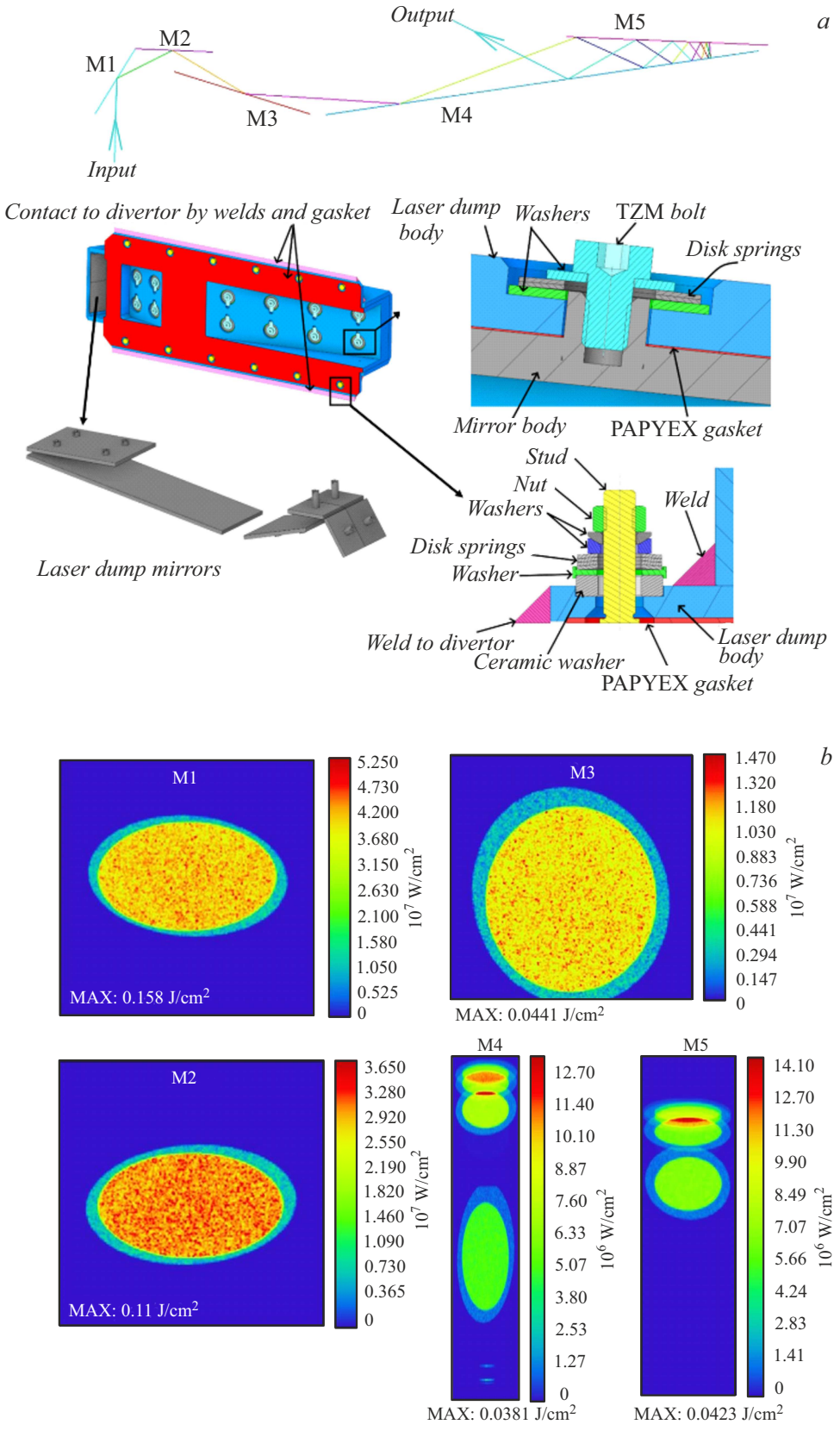

Figure 2. *a* — General view of the laser radiation dump on divertor cassette 21; *b* — distribution of the laser radiation power density on the surface of mirrors M1–M5.

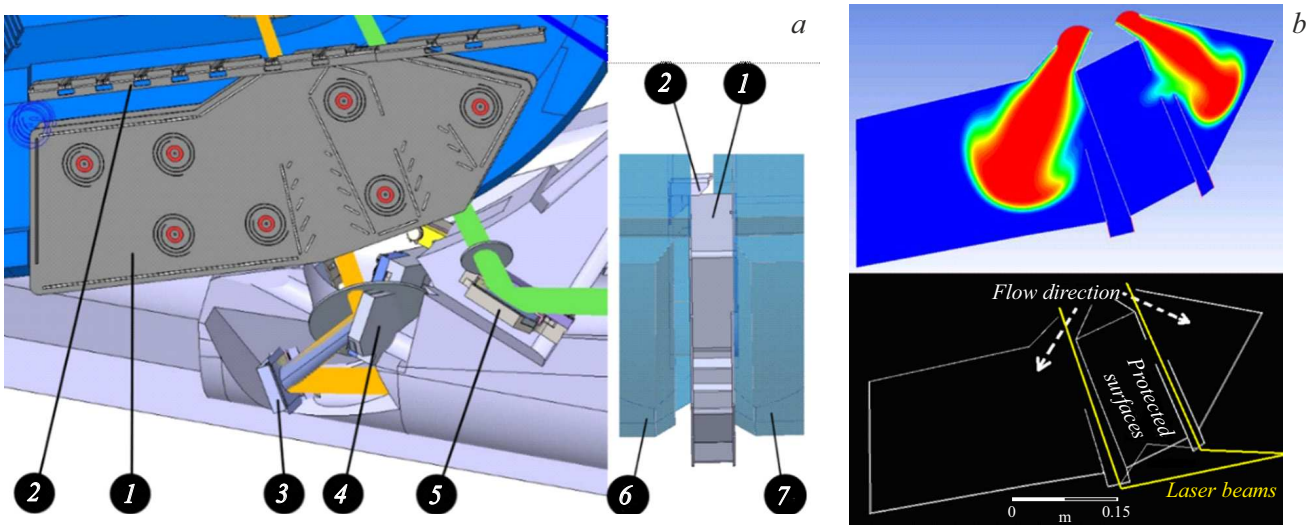

Figure 3. Gasdynamic protection device (dust visor, dust baffle). *a* — general view of the design. *1* — Dust baffle; *2* — dust visor; *3*, *4* — probing chord *A* mirrors; *5* — probing chord *B* mirrors; and *6*, *7* — divertor cassettes 21 and 22. *b* — Principle of operation of the gasdynamic protection device [4].

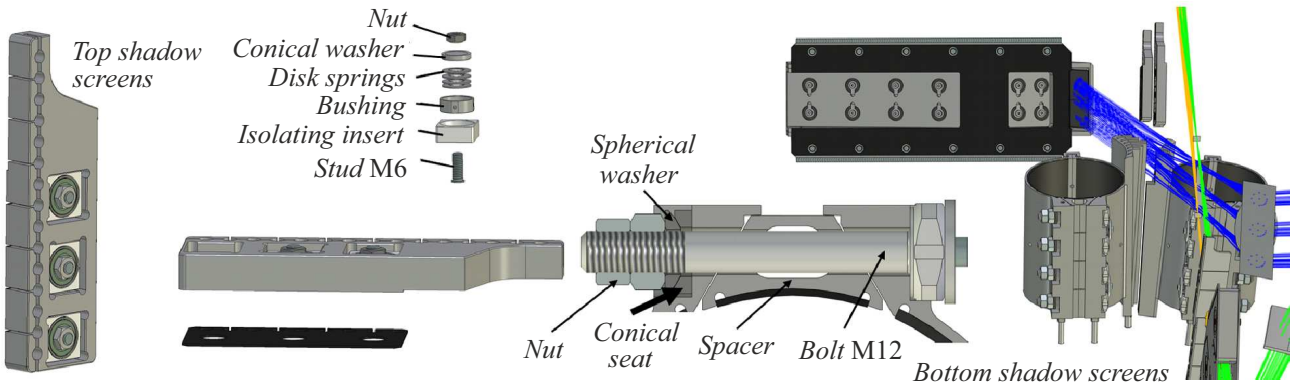

Figure 4. General view of the design of shadow screens and their surroundings.

The laser radiation dump is a device designed to absorb high-power laser radiation (1064 nm/2 J/3 ns/50 Hz) passing along the optical path of laser probing chord *C* and transfer the absorbed heat to the divertor cassette. The dump should withstand intense thermal and electromagnetic loads.

It is secured to cassette 21 with threaded studs and fixed additionally by arc welding in a shielding gas. The general view of the model is presented in Fig. 2, *a*. The design ensures thermal contact with the cooled body of the divertor cassette and positioning of the mirror dump that absorbs high-power laser radiation. The clamping force is produced by a pack of disk springs. To prevent deformation of molybdenum mirror surfaces during normal operation, the design includes independent mounts for mirrors, which allow them to expand freely while maintaining their shape. Carbon washers ensure thermal contact between molybdenum mirrors and the stainless steel body. The optical circuit of the laser radiation dump was designed with account for the dependence of the absorption coefficient on incidence angle and polarization of laser radiation. The trajectory of laser radiation is shown in Fig. 2, *a*.

The authors of [2] have performed a comparative study of laser degradation of polycrystalline and single-crystal molybdenum mirrors using a pulsed Nd : YAG laser with the following operation parameters: 1064 nm/0.5 J/12 ns/10 Hz. It was demonstrated that surface degradation of polycrystalline molybdenum starts with roughness at grain boundaries, which is followed by grain destruction and melting. The comparison of polycrystalline and single-crystal Mo revealed no signs of degradation of the surface of single-crystal molybdenum exposed to $1.5 \cdot 10^6$ pulses with an energy density of 0.9 J/cm^2. Polycrystalline Mo mirrors are susceptible to degradation due to the inhomogeneity of their crystal structure, and the laser damage threshold was measured to be 0.2 J/cm^2 for $1.5 \cdot 10^6$ pulses. With a laser

pulse duration of 3 ns, this translates into $\sim 0.1\,\mathrm{J/cm^2}$ for $1.5 \cdot 10^6$ pulses [3]. According to the calculation results, the energy density of laser radiation at mirrors M3–M5 and M1, M2 does not exceed $0.1\,\mathrm{J/cm^2}$ and $0.16\,\mathrm{J/cm^2}$, respectively (Fig. 2, *b*). Thus, polycrystalline molybdenum may be used to manufacture mirrors M3–M5. Mirrors M1 and M2 must be made of single-crystal molybdenum.

A special channel in the gap between the divertor cassettes is proposed to be used to protect the laser optics for radiation injection into divertor plasma. The surface of the divertor plates is made of tungsten and is coated with boron-containing films during operation. This surface is subject to sputtering, and sputtering products may reach the optical elements of Thomson scattering diagnostics together with gas flows during pressure jumps with a pulse duration of $0.3-01\,\mu$s (the duration of ELM instabilities, where ELM stands for „edge localized mode"). The operation of this structure relies on the following phenomena: (1) the hydrodynamic flow is diverted from the optical axis due to the fact that the channel entrance is oblique with respect to the optical axis; (2) diffusion and convection flows of B and W atoms are absorbed by the channel walls. The operating principle of this device was detailed in [4] (Figs. 3, *a*, *b*).

The gasdynamic protection device is secured permanently to cassettes 21 and 22; bushings with an increased surface area ensure positioning of the mounting studs. The device is involved in protecting the diagnostic system windows from pulsed convective flows [4]. Figure 3, *a* shows the general view of the designed models. The key parts are made of steel sheets that are welded together. The devices are positioned in the gap between divertor cassettes 21 and 22. The main part of the structure features deflectors that direct and distribute convection flows of erosion products inside the device.

Bottom and top shadow screens are mounted opposite each other on the side elements of ITER divertor cassettes 21 and 22. Their purpose is to shield the scattered radiation collection system from thermal radiation of the heated divertor plates of the ITER inner divertor.

The top shadow screens are secured permanently to cassettes 21 and 22. The design of shadow screens is presented in Fig. 4. The split bracket with studs positioned in its holes is the main element of the structure. The main structural material is the TZM (titanium, zirconium, molybdenum) alloy, which has a high melting point ($\sim 2600\,^\circ$C) and is resistant to creep and irradiation (including neutron irradiation). Ceramic elements provide electrical insulation of the structure, reducing significantly the influence of electromagnetic forces induced by eddy currents. The clamping force is produced by a pack of disk springs. Heat is transferred through PAPYEX graphite sheets, which provide thermal contact between the shadow screens and the cooled surface of the divertor cassette. The requirements for mechanical stability of components were taken into account in the design. Thus, the shadow screens have the capacity to counteract vibrations and mechanical stresses during tokamak operation. They are modular, which simplifies their mounting on the divertor cassettes.

The bottom shadow screens are secured with bolts to cassettes 21 and 22 and cover the cooling pipes on which the dome of the divertor cassettes is positioned. The shadow screens have the form of clamps that reproduce the shape of pipes after pressuring. The elastic properties of brackets and graphite gaskets between the shadow screens and the cassette domes compensate for differences in the shape of contact surfaces. The screens are made in the form of multistep ledges that shield against direct and scattered radiation. As before, graphite gaskets ensure thermal coupling. The screens are designed so that the temperature of surfaces within the field of view of the scattered radiation collection system is kept below $500\,^\circ$C, which helps minimize the intensity of background radiation.

The results of development of components of the optical path for Thomson scattering diagnostics mounted on the ITER tokamak divertor cassettes were presented. Particular attention was paid to the structures that provide protection of diagnostic optics from extreme influences, such as radiation, thermal loads, magnetic fields, and electromagnetic loads induced by the interaction of eddy currents, which are produced by the breakdown of a plasma discharge, and a magnetic field of $6-9$ T.

The results of calculations and experiments helped optimize the efficiency of heat removal in the laser radiation dump. Its first mirrors will be made of single-crystal molybdenum, since they should withstand an energy density up to $0.16\,\mathrm{J/cm^2}$ without critical degradation. The design of the gasdynamic protection device, including the dust baffle and dust visor, specifies a spring joint with the divertor cassette, which allows for independent expansion under heating while maintaining thermal contact with the cassette. Screens made of the TZM alloy and PAPYEX graphite gaskets ensure resistance to thermal and electromagnetic loads while maintaining component temperatures below $500\,^\circ$C.

The structures were designed with account for the key requirements of the ITER project as to the reliability of diagnostic systems under long-term operation. It is planned that further research will focus on the optimization of thermal interfaces and the discussed designs in light of the results of subsequent analysis of resistance to seismic, electromagnetic, and thermal loads.

Conflict of interest

The authors declare that they have no conflict of interest.

References

[1] E.E. Mukhin, R.A. Pitts, P. Andrew, I.M. Bukreev, P.V. Chernakov, L. Giudicotti, G. Huijsmans, M.M. Kochergin, A.N. Koval, A.S. Kukushkin, G.S. Kurskiev, A.E. Litvinov, S.V. Masyukevich, R. Pasqualotto, A.G. Razdobarin, V.V. Semenov, S.Yu. Tolstyakov, M.J. Walsh, Nucl. Fusion, **54**, 043007 (2014). DOI: 10.1088/0029-5515/54/4/043007

[2] D.I. Elets, A.G. Razdobarin, A.M. Dmitriev, N.A. Babinov, A.N. Bazhenov, I.A. Khodunov, A.N. Koval, G.S. Kurskiev, A.E. Litvinov, E.E. Mukhin, D.S. Samsonov, V.A. Senichenkov, L.A. Snigirev, V.A. Solovei, I.B. Tereschenko, S.Yu. Tolstyakov, L.A. Varshavchik, P.V. Chernakov, Al.P. Chernakov, An.P. Chernakov, N.S. Zhiltsov, in *Proc. of SOFT 2020* (Dubrovnik, Croatia, 2020).

[3] E. Yatsuka, T. Hatae, G. Vayakis, M. Bassan, K. Itami, M. Walsh, Fusion Eng. Des., **100**, 461 (2015). DOI: 10.1016/j.fusengdes.2015.07.018

[4] I.M. Bukreev, E.E. Mukhin, S.V. Bulovich, A.A. Matyushenko, N.A. Babinov, A.M. Dmitriev, A.E. Litvinov, A.G. Razdobarin, D.S. Samsonov, L.A. Varshavchick, P.A. Zatilkin, J. Phys.: Conf. Ser., **1400**, 077040 (2019). DOI: 10.1088/1742-6596/1400/7/077040

Translated by D.Safin